JACS
JOURNAL OF THE AMERICAN CHEMICAL SOCIETY
Article
pubs.acs.org/JACS

Energetics of Formic Acid Conversion to Adsorbed Formates on Pt(111) by Transient Calorimetry

Trent L. Silbaugh,[†] Eric M. Karp,[†] and Charles T. Campbell*[,†,‡]

[†]Department of Chemical Engineering and [‡]Department of Chemistry, University of Washington, Seattle, Washington 98195, United States

ABSTRACT: Carboxylates adsorbed on solid surfaces are important in many technological applications, ranging from heterogeneous catalysis and surface organo-functionalization to medical implants. We report here the first experimentally determined enthalpy of formation of any surface bound carboxylate on any surface, formate on Pt(111). This was accomplished by studying the dissociative adsorption of formic acid on oxygen-presaturated (O-sat) Pt(111) to make adsorbed monodentate and bidentate formates using single-crystal adsorption calorimetry. The integral heat of molecular adsorption of formic acid on clean Pt(111) at 100 K is 62.5 kJ/mol at 0.25 monolayer (ML). On O-sat Pt(111), the integral heat of the dissociative adsorption of formic acid to make monodentate formate ($HCOO_{mon,ad}$) plus the water−hydroxyl complex ($(H_2O{-}OH)_{ad}$) was found to be 76 kJ/mol at 3/8 ML and 100−150 K. Similarly, its integral heat of dissociative adsorption to make bidentate formate ($HCOO_{bi,ad}$) plus $(H_2O{-}OH)_{ad}$ was 106 kJ/mol at 3/8 ML and 150 K. These heats give the standard enthalpies of formation of adsorbed monodentate and bidentate formate on Pt(111) to be −354 ± 5 and −384 ± 5 kJ/mol, respectively, and their net bond enthalpies to the Pt(111) surface to be 224 ± 13 and 254 ± 13 kJ/mol, respectively. Coverage-dependent enthalpies of formation were used to estimate the enthalpy of the elementary reaction $HCOOH_{ad} \rightarrow HCOO_{bi,ad} + H_{ad}$ to be −4 kJ/mol at zero coverage and +24 kJ/mol at 3/8 ML.

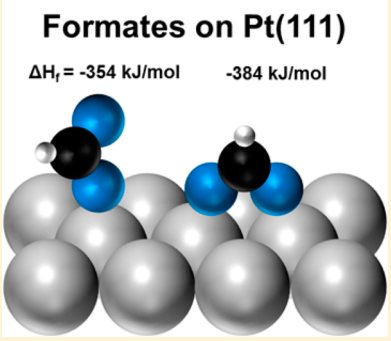

INTRODUCTION

Surface carboxylates, of which formate is the simplest, are common species in many catalytic reactions and are used as linkers for attaching alkyl chains and other organic functional groups to surfaces. Adsorbed formate has been investigated as a potential catalytic intermediate in many catalytic reactions on Pt, including the water−gas shift reaction,[1,2] methanol oxidation, and direct methanol fuel cells,[3−7] and is probably present in many oxidation and steam reforming reactions as well. The surface interactions of organic molecules containing $-COO^-$ and −COOH groups, including amino acid residues, peptides, and proteins, are also important for the organo-functionalization of surfaces,[8] the synthesis of size- and shape-controlled inorganic nanoparticles,[8,9] and their use in medical applications,[10] medical implants,[11] chemical sensors, and many other areas. However, the heat of formation has not been measured for *any* well-defined surface formate nor for *any* other carboxylate on *any* surface. Here, we report experimental measurements of the enthalpies of formation and bond strengths of adsorbed formate in both monodentate and bridge-bonded bidentate bonding configurations on Pt(111), produced by the dissociative adsorption of formic acid. This surface is the most thermodynamically stable face of platinum and therefore the most studied as a model catalyst. The surface interactions of formic acid (HCOOH) itself have been studied due to its potential as a hydrogen storage material[12] and a fuel for direct formic acid fuel cells.[13]

Surface science studies of HCOOH adsorption on Pt(111) have found that, when the surface is predosed with oxygen adatoms, formic acid deprotonates to form adsorbed formate ($HCOO_{ad}$), OH_{ad}, and/or H_2O_{ad}.[14−16] The OH_{ad} product in those studies was assigned based on comparison to vibrational spectra for OH_{ad} produced by dosing water to oxygen-dosed Pt(111), which was later proven to actually be a $(H_2O{-}OH)_{ad}$ complex,[17,18] so this $(H_2O{-}OH)_{ad}$ complex is the most likely product, rather than OH_{ad} alone as originally proposed. Adsorbed formate has been observed in the monodentate structure on Pt(111), which then converts to the more stable bridge-bonded bidentate formate at higher temperature.[14] Carboxyl (−COOH) has been suggested by density functional theory (DFT) calculations to be an important but unstable intermediate on Pt in many reactions, most notably water−gas shift.[1,2] However, it has never been observed experimentally, probably because it quickly converts to other species. So, while it might be produced in very small concentrations after dosing HCOOH to O/Pt(111), formates are the dominant products of that stoichiometry. This is consistent with the relative instability of carboxyl compared to formates on Pt(111) predicted by DFT.[1,2]

Knowledge of fundamental thermodynamic information, especially the enthalpies of formation of adsorbed species on metal surfaces, allows us to better understand complex reaction mechanisms occurring on catalytic surfaces. The difficulty of obtaining this information experimentally is that the usual techniques (e.g., temperature programmed desorption (TPD)

Received: December 18, 2013
Published: February 10, 2014

   dx.doi.org/10.1021/ja412878u | *J. Am. Chem. Soc.* 2014, 136, 3964−3971

and equilibrium adsorption isotherms) require adsorbates to desorb reversibly. However, many adsorbates further react or decompose prior to desorption, thus limiting the utility of those techniques. As a result, experimentally determined enthalpies of formation of adsorbed molecular fragments and their adsorbate−surface bond enthalpies are still rarely available. An ultrahigh vacuum technique that can directly measure the heat released upon adsorption, known as single-crystal adsorption calorimetry (SCAC), was developed in King's group at Cambridge to overcome this problem[19,20] and has been further improved by our group.[21,22] This technique has been shown to be useful for determining the heat of many types of adsorption reactions, whether molecular, dissociative, reversible, or irreversible.[18,23−27] It has also been shown recently that an analysis of the heat detector's signal line shape in SCAC can provide kinetic information for reactions occurring on the same time scale as the measurements (10−1000 ms).[28]

In this study, we investigated the adsorption of formic acid on clean and oxgyen-presaturated (O-sat) Pt(111) using SCAC between 100 and 190 K. From these heat measurements, we were able to extract the enthalpies of formation and bond strengths of adsorbed formate in both monodentate and bidentate bonding configurations on Pt(111), as well as that for molecularly adsorbed formic acid.

EXPERIMENTAL SECTION

Experiments were performed in an ultrahigh vacuum (UHV) chamber (base pressure $<2 \times 10^{-10}$ mbar) with capabilities for single-crystal adsorption microcalorimetry and surface analysis, as described previously.[22,29] Briefly, the chamber is equipped for X-ray photoelectron spectroscopy (XPS), Auger electron spectroscopy (AES), low-energy ion scattering spectroscopy (LEIS), and LEED. The sample was a 1 μm thick Pt(111) single-crystal foil, supplied by Jacques Chevallier at Aarhus University in Denmark. The sample cleaning procedures that were used in this study are described elsewhere.[30] A detailed description of the experimental principles and implementation of the molecular beam flux, sticking probability and heat measurements can be found elsewhere.[22,29,30] Briefly, the Pt(111) sample was exposed to a pulsed molecular beam of formic acid. Each pulse was 102 ms long and repeated every 2.0 s at 100 K and every 5.0 s at 150 and 190 K. After loading formic acid (Fisher Chemical, Optima LC/MS ≥99.5%) into a glass reservoir under N_2 atmosphere and subsequent mounting on the vacuum chamber, the liquid was outgassed by five freeze−pump−thaw cycles. Its purity was verified with a mass spectrometer in the UHV chamber and compared with spectra obtained with gas chromatography−mass spectrometry. Also, water was proven to be below the detection limit of 1% in the starting HCOOH using NMR, consistent with the manufacturer's claim. The beam was created by expanding ∼2 mbar of formic acid through a microchannel array and then collimated through a series of five liquid nitrogen cooled orifices. The microchannel array was heated to 360 K to reduce gas-phase dimerization to less than 1%.[31] This was verified by mass spectrometry by monitoring the ratio of the m/e 29 and 47 signals[32] as a function of microchannel temperature. Pulses were created by mechanically chopping the beam using a rotating disk that has had a small slit removed.

Surface coverages are reported here in monolayers (ML) and are defined as the number of formic acid molecules which adsorb onto the surface irreversibly, independent of the actual species they form on the surface following adsorption. We define one monolayer (ML) of adsorbate coverage as being equal to the density of Pt atoms in the Pt(111) surface (1.50×10^{19} m^{-2}). A typical formic acid pulse is 0.0095 ML ($\sim 2 \times 10^{12}$ molecules).

The flux of formic acid from the molecular beam is measured by impinging the beam onto a liquid nitrogen cooled quartz crystal microbalance (QCM). A unity sticking probability of formic acid onto the QCM was ensured by precovering the QCM with multilayers of formic acid. Calibration of the QCM has been described previously.[22] The heat released from the adsorption of one formic acid pulse to the sample surface is measured with a pyroelectric polymer ribbon gently pressed against the back side of the platinum sample, as described previously.[29] The indicated references provide a more in-depth discussion of heat transfer between sample and ribbon.[33]

The sensitivity of the pyroelectric detector was calibrated after each experiment by depositing pulses of a known amount of energy into the sample using a HeNe (632.8 nm) laser, as described previously.[29] The error in absolute accuracy of the calorimetric heats (after averaging >5 runs) is estimated to be less than 3% for systems like those studied here that have sticking probabilities above 0.8, based on comparisons of our measurements to literature values when forming multilayers with known energies for four different molecules.[25] (This error is due to possible errors in the absolute flux, heat signal calibrations and in the literature values.) Relative measurements (e.g., differences in heat with increasing coverage) are much more accurate, due to the high precision in heat measurements within a run. The sample temperature was controlled during calorimetry as described previously.[34]

The time scale of our heat measurement is comparable to the beam-pulse duration (∼100 ms). If the molecular adsorption/reaction process occurs on a time scale of ∼10 ms or less, the heat signal line shapes measured during molecular and laser pulses are identical, allowing for the comparison of the peak heights or instantaneous slopes to extract the deposited energy from a molecular pulse.[21,30] Heat deposited on a time scale of ∼10 ms or longer results in broadening of the detector response line shape. The detector response of formic acid pulses on clean Pt(111) at 100 K were not broadened with respect to the laser calibration. At 100 and 150 K on O-sat Pt(111), a secondary heat deposition process occurred with a time constant of ∼170 and ∼130 ms, respectively, at all coverages, requiring a more complex data analysis method as described previously.[28] At 190 K on O-sat Pt(111), a slight pulse sharpening occurred due to water desorption with a time constant of ∼600 ms, which was sufficiently slow to not affect the initial slope of the pulse shape.

The Pt(111) surface was exposed to a chopped molecular beam of formic acid, and the sticking probabilities and the heats of adsorption were measured as a function of formic acid coverage. A mass spectrometer was used to monitor the background pressure increase of formic acid (m/e = 46) in the chamber. A room-temperature gold flag was positioned in front of the sample and used to determine the mass spectrometry signal corresponding to full reflection of formic acid. The sticking probability is calculated by comparing the time-integrated mass spectrometer signals measured from the increase in formic acid partial pressure above background from molecular beam pulses onto the sample surface and onto the inert gold flag. We report two types of sticking probabilities: the long-term sticking probability, which is defined as the probability that molecules in a gas pulse stick during the full duration of the pulse repeat period (5 s), and the short-term sticking probability, which is defined as the probability that molecules in a gas pulse stick on the surface until the end of the ∼140 ms time period used to measure the heat signal, measured as described previously.[30] The long-term sticking probability is used to calculate the coverage at the start of the next pulse, and the short-term sticking probability is used to calculate adsorption energies per mole adsorbed.

Due to the transient sticking of a small amount of formic acid on the vacuum chamber walls, a slightly different procedure from that described in the paper cited above was required to measure these sticking probabilities. These sticking probabilities were measured using both the true King and Wells method with nonline-of-sight (NLOS) detection[35] and a modified King and Wells method that uses line-of-sight (LOS) detection.[21] For the modified King and Wells method, the flag blocking LOS to the mass spectrometer was removed, giving direct LOS to the sample.

The results from these two types of sticking probability measurements showed two minor but significant differences:

(1) When the sticking probabilities were constant and not changing with time, the value detemined from the LOS measurements

were found to differ slightly in absolute magnitude from the NLOS measurements due to the different temperatures of the sample and gold flag and their different positions relative to the mass spectrometer ion source, which lead to errors in the nonsticking reference signal in the LOS measurements, not present in the NLOS measurements. Since the NLOS measurements give the true value for the nonsticking fraction, the LOS measurements of this fraction can be scaled to the true NLOS value.

(2) When the surface saturates, there is often a sharp decrease in the sticking probability or an increase in the nonsticking fraction measured. This increase in the mass spectrometer signal was always observed to occur several pulses sooner using LOS than the NLOS measurements. This delay in the NLOS signal is attributed to the transient consumption of a small amount of formic acid by the chamber walls. The result is a higher apparent saturation coverage in the NLOS measurements. This does not occur in LOS measurements, since the majority of detected molecules do not contact the chamber walls.

Thus, neither sticking probability measurement is completely accurate except when $S = 1$, since both the LOS and NLOS measurements would lead to one type error or the other. The NLOS measurements are accurate in absolute value when S is constant (i.e., at both low and high coverages) but not when S is rapidly decreasing. We therefore use the LOS values here but scale their magnitude so that they agree with the sticking probabilities from the NLOS data at coverages where S is constant.

RESULTS

Sticking Probability. The short- and long-term sticking probabilities of formic acid on clean and O-sat Pt(111) were measured at several temperatures, as shown in Figure 1. Here,

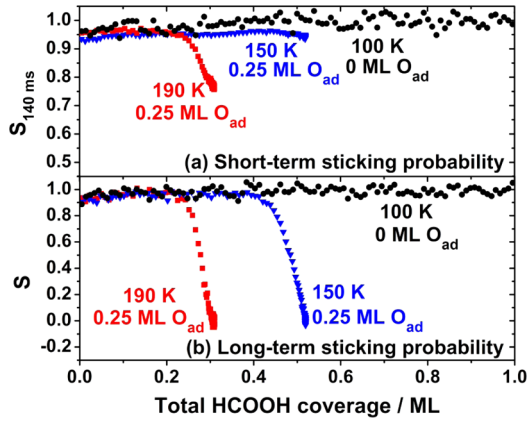

Figure 1. (a) Short-term and (b) long-term sticking probabilities of formic acid on clean Pt(111) at 100 K and O-saturated Pt(111) at 150 and 190 K as a function of the total formic acid coverage that adsorbed (irrespective of its final structure after adsorption). Although not shown, the sticking probabilities at 100 K on O-saturated Pt(111) were very similar to those shown here on clean Pt(111) at 100 K.

O-sat Pt(111) refers to a Pt(111) surface covered with 0.25 ML of oxygen adatoms. The sticking probabilities at 100 K were obtained using NLOS data only, while those for 150 and 190 K were measured using the LOS data but scaled using the NLOS data as described above. The initial sticking probabilities are high (>0.9) at all temperatures, and their constant or even increasing values with coverage indicate a precursor-mediated adsorption mechanism.[25] The increase in sticking probability over the first 0.25 ML is due to mass matching between adsorbates and incoming molecules and has been observed previously for both H_2O[18,36] and methanol[25] on O-sat Pt(111). A clear temperature dependence of the saturation coverage of formic acid on Pt(111) can be seen in Figure 1. At 100 K, formic acid continues to populate a multilayer state upon saturating the surface. However at 150 K, the sticking probability decreased rapidly above 0.4 ML and dropped to zero at 0.52 ML. This lack of multilayer growth at 150 K is consistent with TPD results that report a multilayer desorption peak beginning at ~130 K and peaking at 160−170 K.[15] The sticking probability at 190 K begins decreasing sharply at 0.25 ML and reaches zero at a saturation coverage of 0.31 ML.

Heats of Adsorption. From the literature, it is known that formic acid adsorbs molecularly on clean Pt(111) at 100 K.[16,32] Our measurements at 100 K (Figure 2) show that the initial

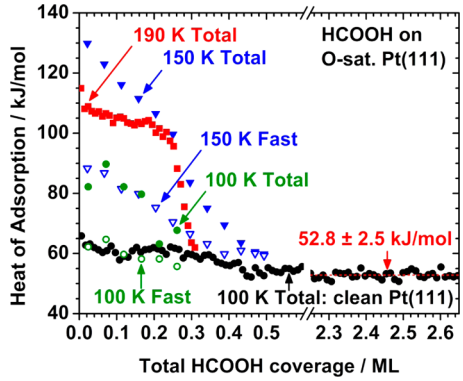

Figure 2. Heats of adsorption measured at various temperatures on clean Pt(111) at 100 K (black circles) and O-saturated Pt(111) at 100 K (hollow and solid green circles), 150 K (hollow and solid blue triangles), and 190 K (red squares) as a function of total coverage of adsorbed HCOOH, irrespective of its final structure. Hollow symbols represent fast heat deposition steps while solid symbols represent total heats (i.e., the sum of fast and slow steps). The multilayer heat of adsorption is indicated by a dotted line through the 100 K data in the lower right corner.

heat of formic acid molecular adsorption is 65 kJ/mol and drops slowly to 60 kJ/mol at 0.25 ML. From 0.25 to 0.5 ML, the heat of adsorption decreases more quickly, falling to 52.8 ± 2.5 kJ/mol at 0.5 ML. This coverage of 0.5 ML (7.5×10^{18} molecules/m^2) is similar to the saturation coverages of both the α and β phases of formic acid adsorbed on graphitized Ni(110), where molecule−surface interactions are minimal, of 7.0 and 6.2×10^{18} molecules/m^2 respectively.[37] The slightly higher packing density seen here may be due to the stronger binding to, and the packing density and geometry of sites on, the Pt(111) surface. The heat above 0.5 ML remains level at 52.8 ± 2.5 kJ/mol as subsequent layers are populated.

We can compare this multilayer heat to multilayer desorption of formic acid from TPD data available in the literature.[32] We estimate an activation energy for desorption of 50 kJ/mol from the reported peak temperature of 170 K[32] using simple first-order Redhead analysis.[38] For this, we estimated a prefactor of $10^{15.4}$ s^{-1} following the entropy method developed by Campbell and Sellers[38,39] using the gas-phase entropy of formic acid at 170 K of 248.7 J/(mol K).[40] To compare this TPD value to our results, we must also add to it 1/2 RT, giving 51 kJ/mol. The agreement is quite good, with this TPD value falling within the error of our measurements. This confirms the absolute accuracy of our calorimetric heats.

dx.doi.org/10.1021/ja412878u | J. Am. Chem. Soc. 2014, 136, 3964−3971

Below 143 K, adsorption of formic acid at high coverage results in the formation of an amorphous multilayer rather than the more stable crystalline α phase.[41,42] Our measured heat of adsorption at 100 K therefore corresponds to the binding of formic acid in an amorphous multilayer and is consequently lower than the heat of sublimation of ~60.5 kJ/mol[43] obtained above 200 K for the crystalline α phase.

In order to describe the calorimetry results obtained at 100 and 150 K on O-sat Pt(111), we must first describe a new heat detector signal-line shape analysis method developed in our lab.[28] The necessity for this new method comes from the observation that, if all, or some fraction, of heat deposition from molecular adsorption occurs on a time scale of 10−1000 ms for a pulse length of ~102 ms, a visible broadening of the detector response pulse for molecular adsorption is seen relative to the laser calibration response.[28]

The following is a brief description of this analysis method, which is described in detail elsewhere.[28] This method involves fitting the detector response using a two-step reaction sequence with a single rate-limiting step. The first step is fast, and its heat is deposited on a time scale much faster than the pulse duration, as is common, for example, in simple molecular adsorption. Since it is fast, its heat signal pulse line shape is well represented by the line shape obtained from the laser heat calibration experiment. The second step is slower and deposits heat on the same time scale of the heat measurement. This can be due to activated dissociation of an adsorbed molecule or some activated conversion of some quickly adsorbed molecular fragment (for example, the conversion of monodentate formate to bidentate fomate). It is responsible for the observed pulse broadening and is fit using the laser calibration line shape convoluted with an exponential decay for a first-order reaction. The time constant of this exponential decay is a fitting parameter and is equal to the inverse of the reaction rate constant for this process. The fraction of heat in each of these two steps and the time constant are adjusted until the simulated pulse (SP) (sum of the two pulse lineshapes) best fits the experimental heat pulse (EH). From this analysis method, we are able to obtain heats of adsorption for the first step (labeled "Fast" in Figure 2) and the sum of the first and second steps (labeled "Total" in Figure 2) as well as the reaction time constant, τ, for the slow second step.

A representative broadened detector line shape is shown in Figure 3 along with the best-fit simulated pulse obtained from the sum of pulse lineshapes representing fast (S1) and slow (S2) heat deposition processes. This particular pulse was obtained for formic acid adsorption on O-sat Pt(111) at 150 K and was well fitted with a S1 heat of 79 kJ/mol, S2 of 36 kJ/mol, and τ of 100 ms (k = 10 s^{-1}). For this analysis method, groups of five consecutive pulses were averaged to improve signal-to-noise. As a consequence, the heat data points reported for the 100 and 150 K experiments represent doses of 0.0475 ML. The negative voltage region in these signals is due to the detector preamplifier (which has both integrating and differentiating components) and is seen with laser pulses as well. It does not indicate an endothermic process.

As was observed for methyl iodide adsorption on Pt(111) at 270 K,[26,28] dosing of formic acid on O-sat Pt(111) at 100 and 150 K resulted in noticeably broadened pulse lineshapes. Pulseshape analysis therefore provides two heats of adsorption ("fast" and "total") for each pulse.

Dosing of formic acid on O-sat Pt(111) at 100 K results in fast heats of adsorption that are similar to those seen on the clean Pt(111) surface (Figure 2). This is consistent with calorimetry experiments of H_2O adsorption on clean and O-sat Pt(111) at 100 K, where the heats of molecular adsorption of H_2O were nearly unaffected by the presence of adsorbed oxygen atoms (increasing by only 3.7 kJ/mol).[36] The initial fast heat of adsorption (i.e., at the zero coverage limit) is 65 kJ/mol and decreases linearly with increasing coverage. However, unlike the H_2O experiments, a second, slower reaction (with a τ of 170 ± 19 ms) deposits additional heat here, of magnitude almost 30 kJ/mol initially but decreasing with coverage. The initial total heat of adsorption of formic acid on O-sat Pt(111) at 100 K is the sum of the heats for these two steps, or ~90 kJ/mol initially followed by a linear decrease with coverage. The data shown in Figure 2 at 100 K on O-sat Pt(111) is the average of three experiments.

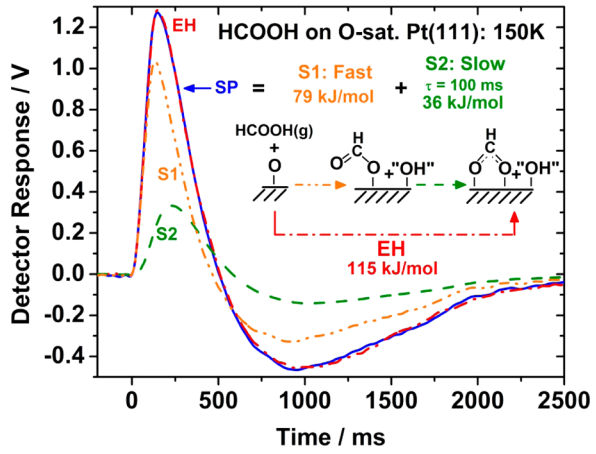

Figure 3. Experimental and simulated pulses obtained from a best-fit analysis of formic acid on O-sat Pt(111) at 150 K. The experimental heat-signal pulse (EH) is an average over the coverage range 0.13−0.18 ML. The simulated pulse (SP) fits EH so well that the curves can barely be distinguished. This confirms the accuracy of the parameters (i.e., S1 and S2 heats and the slow step time constant, τ) obtained from this analysis. The species "OH" here is short for the water−OH complex, with the stoichiometry really being that of reaction 4.

Dosing of formic acid on O-sat Pt(111) at 150 K results in fast heats of adsorption that are similar to the total heats measured on the O-sat Pt(111) surface at 100 K. This makes sense, since any chemical step with a τ of 170 ms at 100 K should be much faster than the time scale of the experiment (i.e., <10 ms) already at 150 K. The heat of adsorption, initially 91 kJ/mol, decreases linearly with increasing coverage and eventually falls to 60 kJ/mol at a coverage of 0.4 ML (Figure 2). The heat remains constant at 60 kJ/mol up to 0.5 ML. As seen at 100 K on O-sat Pt(111), this fast heat deposition is followed by a second slow process, this time with a τ of 130 ± 13 ms. The total heat of adsorption in the limit of zero coverage is 131 kJ/mol and decreases linearly to 100 kJ/mol at 0.25 ML. This is followed by a slightly sharper drop between 0.25 and 0.3 ML (100 to 84 kJ/mol) and then a slow linear decrease between 0.3 and 0.5 ML, eventually ending at 60 kJ/mol. The data shown in Figure 2 at 150 K on O-sat Pt(111) are the average of five experiments.

Formic acid dosed on O-sat Pt(111) at 190 K exhibits a linearly decreasing heat of adsorption up to 0.25 ML. A linear fit to this data gives the equation (110−45.8θ) kJ/mol, where θ is the total HCOOH coverage in ML. Between 0.25 and 0.31 ML, a much sharper linear decrease is seen, falling from a heat

dx.doi.org/10.1021/ja412878u | J. Am. Chem. Soc. 2014, 136, 3964−3971

of adsorption of 99 kJ/mol at 0.25 ML to 60 kJ/mol at 0.31 ML.

DISCUSSION

Formic Acid Chemistry on Clean and O-Sat Pt(111). To interpret the above results, we must first discuss the temperature-dependent chemistry of formic acid on O-sat Pt(111). The reactions posed in the following paragraphs are drawn from the existing body of literature as well as observations from the current report.

As already discussed, formic acid molecularly adsorbs on clean Pt(111) at 100 K[32] as given by the following reaction:

$$HCOOH_g \rightarrow HCOOH_{ad} \quad (1)$$

However on the O-sat Pt(111) surface, high-resolution electron energy loss spectroscopy (HREELS) was used to show that formic acid deprotonates at 100 K.[15] This promotion of deprotonation by adsorbed atomic oxygen has been observed previously for formic acid, alcohols, and other acids (e.g., methanol and acetic acid) on several metal surfaces (e.g., Pt(111),[15,16,44] Cu(110),[45] Rh(111),[46] Ag(110)[47]).

This loss of the acid proton of HCOOH was reported to lead to the formation of *both* monodentate and bidentate formate adsorbed to Pt(111) at 100 K.[15] However, in that study, the authors assigned the dual peaks at 1330 and 1630 cm^{-1} (the two peaks were of nearly equal magnitude) to the presence of bidentate and monodentate formate, respectively, citing earlier work by Avery.[14] These assignments are inconsistent with the cited report by Avery,[14] which assigned two peaks of equal magnitude at 1290 and 1620 cm^{-1} to the presence of *only* monodentate formate. It is also important to note that these experiments that initially observed the monodentate formate species, performed at 130 K, found that the monodentate species was stable on the order of minutes, converting to a bidentate formate species in the time it took to run a second HREELS scan (~10 min). It seems unlikely that a monodentate species would convert to a bindentate configuration at 100 K if the conversion was observed to be so slow at 130 K. We therefore conclude that formic acid deprotonates to form *only* monodentate formate at 100 K.

The presence of hydroxyl groups was observed for low and high submonolayer coverages of formic acid at 170 and 130 K respectively, consistent with the observed low-coverage water desorption peak at 205 K in TPD arising from the recombination of adsorbed −OH groups.[15] This TPD peak broadened to lower temperatures with increasing formic acid coverage, eventually exhibiting a peak maximum characteristic of the desorption of pure adsorbed H_2O at 170−175 K. This explains why only this low temperature TPD peak (180 K) was observed by Avery, as his experiments were performed at much higher formic acid coverages.[16] We therefore adopt the reaction scheme below, whereby adsorbed oxygen and then hydroxyl are sequentially protonated by the acid H of HCOOH. At low coverage, formic acid first adsorbs molecularly:

$$HCOOH_g + O_{ad} \rightarrow HCOOH_{ad} + O_{ad} \quad (2)$$

and then donates its acid proton to adsorbed oxygen to form adsorbed monodentate formate and hydroxyl:

$$HCOOH_{ad} + O_{ad} \rightarrow HCOO_{mon,ad} + OH_{ad} \quad (3)$$

However, it is well known that OH_{ad} on Pt(111) quickly converts to a $(H_2O{-}OH)_{ad}$ complex at 150 K and above,[18] so that the net reaction observed at low coverages and 150 or 190 K is then the more complex reaction:

$$3HCOOH_g + 2O_{ad} \rightarrow 3HCOO_{mon,ad} + (H_2O{-}OH)_{ad} \quad (4)$$

Although this $(H_2O{-}OH)_{ad}$ complex is quickly formed by dosing water to O_{ad} on Pt(111) at 150 K, it is not yet formed at 100 K.[18,36] However, it might be formed by dosing HCOOH to O_{ad} at 100 K, and our heat results suggest it does, as discussed below. The production of coadsorbed water has already been proposed for the reaction of adsorbed formic acid with atomic oxygen on Pt(111),[15] Ag(110),[47] and Rh(111).[46]

Given that the saturation coverage of O_{ad} on Pt(111) is 0.25 ML, reaction 4 can proceed to a coverage of 0.375 ML of adsorbed formate. This is consistent with the coverage where the heats drop to that characteristic of molecular adsorption at 150 and 190 K in Figure 2, given that this drop may be broadened by heterogeneity in local surface coverage.

As noted previously, a slow transition to bridge-bonded bidentate formate was observed at 130 K by HREELS,[14] as given by

$$HCOO_{mon,ad} \rightarrow HCOO_{bi,ad} \quad (5)$$

At 150 K and above, reaction 4 will therefore be followed by reaction 5, ultimately giving the net reaction

$$3HCOOH_g + 2O_{ad} \rightarrow 3HCOO_{bi,ad} + (H_2O{-}OH)_{ad} \quad (6)$$

at saturation.

Mass spectrometry measurements of the water signal (not shown) revealed the desorption of a water pulse following each formic acid pulse at 190 K on O-sat Pt(111) at low coverages. This water pulse had a tail that was reasonably well fit by an exponential decay with a time constant of ~100 ms. This is consistent with the report that water is stable in the water−OH complex on Pt(111) at 150 K but shows significant desorption within 2 s at higher temperatures.[18] Similarly, HREELS experiments after dosing HCOOH to O_{ad} on Pt(111) observed the disappearance of H_2O_{ad} upon heating to 190 K.[14,15] Therefore, at 190 K, some water desorption must also be considered in analyzing the heat data.

We can now discuss our calorimetry results in the context of known formic acid chemistry on Pt(111), by assigning particular reactions to each heat of adsorption curve (Figure 2). As discussed earlier, both the total heat on clean Pt(111) at 100 K and the fast heat on O-sat Pt(111) at 100 K can be assigned to molecular adsorption, as given by either reaction 1 on clean Pt(111) or reaction 2 on O-sat Pt(111), respectively. On the O-sat surface, a second, slow heat deposition is also seen and can be assigned to the deprotonation of formic acid via reaction 3 at low coverage and 100 K.

At 150 K, the deprotonation of $HCOOH_{ad}$ to form OH_{ad} is much faster than the time scale of our measurement. As noted above, the water−OH complex is also quickly formed at this temperature. Thus, we assign the fast heat at 150 K to reaction 4 up to 0.375 ML. The agreement between the fast heats at 150 K and the total heats at 100 K on O-sat Pt(111) indicate that we can also assign the total heats at 100 K to reaction 4 up to 0.375 ML. As expected from HREELS, a second, slower step is observed at 150 K that we can assign to the subsequent conversion of monodentate to bidentate formate, reaction 5. The total heats at 150 K therefore correspond to the sum of reactions 4 and 5, that is, net reaction 6, up to 0.375 ML.

dx.doi.org/10.1021/ja412878u | J. Am. Chem. Soc. 2014, 136, 3964−3971

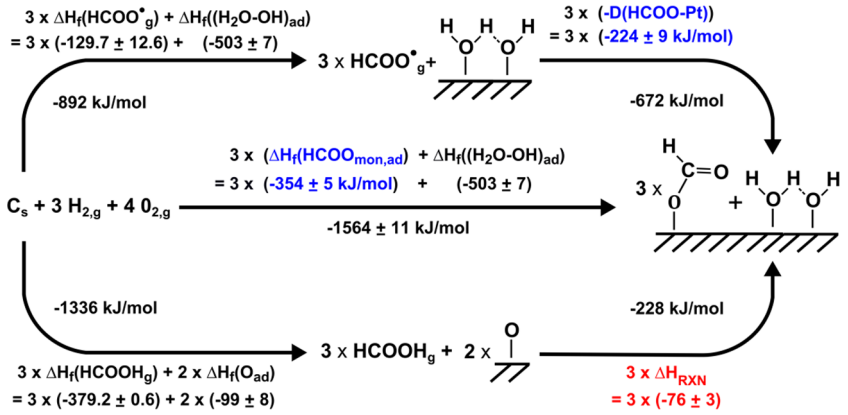

Figure 4. Thermodynamic cycle used to determine the enthalpy of formation of adsorbed monodentate formate on Pt(111) and its HCOO–Pt(111) bond enthalpy from the integral fast S1 heat of adsorption at 150 K and 3/8 ML, shown as the bottom right-hand step. References for literature values are listed in the text.

At 190 K, the net reaction should also be reaction 6. However, because the desorption of H_2O during each pulse occurs with a time constant (~100 ms) comparable to the time used for heat measurement (140 ms), some fraction of H_2O desorbs during heat detection, and the rest remains adsorbed. This means that the total heats of adsorption instead represent a combination of reaction 6 but with some fraction of the $(H_2O{-}OH)_{ad}$ complex decomposing to release water vapor. This is clear in the initial (low coverage) total heats of adsorption that are ~15–20 kJ/mol lower at 190 K than at 150 K. We attribute this to the fact that some of the water desorb at 190 K from the water–OH complex (which has a heat of adsorption of ~60 kJ per mole of water when formed from water vapor plus O_{ad}[18]). Because the stoichiometry of reaction 6 requires three formic acid molecules to make one $(H_2O{-}OH)_{ad}$, and each $(H_2O{-}OH)_{ad}$ produces $^3/_2$ H_2O_g molecules upon thermal decomposition, only half of this 60 kJ/mol (i.e., 30 kJ/mol) is consumed by water desorption per formic acid molecule adsorbed. The measured initial heat at 190 K is only 15–20 kJ/mol lower than at 150 K, implying that only about 50–65% of the $(H_2O{-}OH)_{ad}$ complex decomposes in the time of the heat measurement at 190 K. Note also that the difference between the heats at 190 versus 150 K decreases with increasing formic acid coverage until it drops to zero at a coverage of 0.25 ML.

Enthalpies of Formation of Monodentate and Bidentate Formate on Pt(111). As discussed above, our measurements represent the heats of reaction upon formic acid adsorption. Using available literature values for the heats of formation of various gas-phase and adsorbed molecules, we can use these measured heats of reaction to determine the enthalpies of formation of adsorbed formate (both monodentate and bidentate) and the HCOO–Pt(111) bond enthalpies.

On the basis of the above discussion, the integral heat of fast adsorption at 3/8 ML and 150 K (76 kJ/mol from integrating the curve in Figure 2) corresponds to the complete consumption of adsorbed oxygen to form adsorbed monodentate formate and the water–hydroxyl complex (reaction 4). Figure 4 shows how to combine this heat in a thermodynamic cycle with other known literature values to calculate the enthalpy of formation of monodentate formate ($\Delta H_f(HCOO_{mon,ad})$). The bottom path starts with elements in their standard state. The bottom left arrow uses the enthalpies of formation of gas-phase formic acid (−379.2 ± 0.6 kJ/mol)[48] and adsorbed atomic oxygen.[49] The enthalpy of formation of atomic oxygen used here is calculated using the integral heat of dissociative O_2 adsorption at 0.25 ML coverage (−99 ± 8 kJ/mol O).[49]

Note that all positive heats of adsorption in Figure 2 represent exothermic processes. In this section, all positive heats of adsorption have been converted to negative enthalpies of reaction for use in thermodynamic cycles. The bottom right-hand arrow in Figure 4 represents our measurement, with an integral enthalpy of reaction of −76 kJ/mol (the fast reaction only at 150 K and 3/8 ML).

The central path in Figure 4 takes elements from their standard states directly to the adsorbed products. The central path must equal the sum of the two steps in the bottom path, thus allowing us to calculate the standard enthalpy of formation of monodentate formate, $\Delta H_f(HCOO_{mon,ad})$, to be −354 kJ/mol, using the known enthalpy of formation of adsorbed water–hydroxyl complex ($\Delta H_f((H_2O{-}OH)_{ad})$), −503 kJ/mol.[49]

Similarly, we can use this thermodynamic cycle to calculate the Pt–O bond enthalpy for adsorbed monodentate formate. The upper left arrow in Figure 4 proceeds from elements in their standard state to the gas-phase formate radical and $(H_2O{-}OH)_{ad}$ using the enthalpies of formation of the formate radical (−129.7 ± 12.6 kJ/mol)[50] and $\Delta H_f((H_2O{-}OH)_{ad})$ (−503 ± 7 kJ/mol). The only unknown in the complete upper path is the arrow representing the negative of the HCOO–Pt(111) adiabatic bond dissociation enthalpy (D(Pt–OOCH)), which is then calculated as 224 kJ/mol.

Using the integral <u>total</u> heat up to 3/8 ML at 150 K (−106 kJ/mol) rather than the fast S1 heat as in Figure 4 (−76 kJ/mol), we can use the same methodology to calculate $\Delta H_f(HCOO_{bi,ad})$ and the $HCOO_{bi}$–Pt(111) bond enthalpy for bidentate formate, where the only difference to Figure 4 is the number of O–Pt bonds created (two rather than one) and the measured heat. This gives the enthalpy of formation of bidentate formate ($\Delta H_f(HCOO_{bi,ad})$) to be −384 kJ/mol and the net bond enthalpy of $HCOO_{bi,ad}$ to the Pt(111) surface to be 254 kJ/mol, or 127 kJ/mol for each of the two Pt–O bonds. Note that this is almost 100 kJ/mol less than the single Pt–O bond enthalpy for monodentate formate above.

Similarly, we can calculate the enthalpy of formation and HCOO–Pt(111) bond enthalpy for monodentate and

dx.doi.org/10.1021/ja412878u | J. Am. Chem. Soc. 2014, 136, 3964–3971

bidentate formate at intermediate coverages using the integral heat between 0 and 0.375 ML total HCOOH coverage, where some fraction of the 0.25 ML of adsorbed oxygen has been consumed via reaction 4. As seen in Figure 5, this allows us to

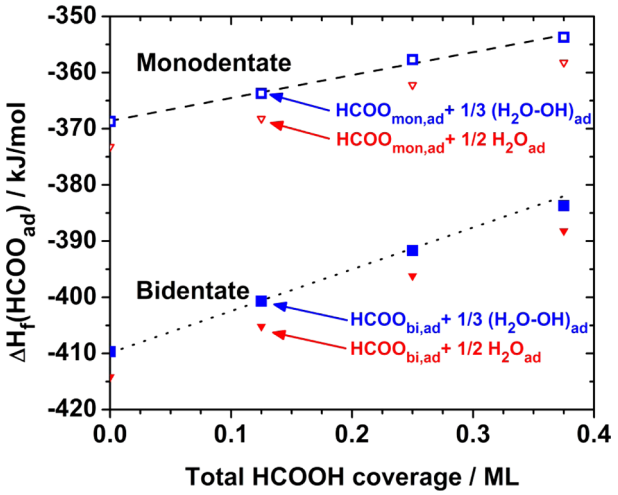

Figure 5. Enthalpy of formation of adsorbed monodentate and bidentate formate species ($\Delta H_f(HCOO_{ad,mon})$ and $\Delta H_f(HCOO_{ad,bi})$, respectively) as a function of total formic acid coverage. The enthalpies of formation of formate are determined using integral heats of reaction measured at 150 K on O-sat Pt(111) along with other known enthalpies of formation in a thermodynamic cycle as shown in Figure 4. The listed coadsorbates (i.e., $(H_2O{-}OH)_{ad}$ and H_2O_{ad}) refer to the stoichiometry used in the thermodynamic cycles.

calculate the coverage-dependent enthalpy of formation of monodentate and bidentate formate. If we calculate these enthalpies assuming either reactions 4 or 6 for the fast or total heat at 150 K respectively, we obtain values indicated by blue square symbols in Figure 5. Linear fits to this data provide equations for the coverage dependent enthalpy of formation of monodentate formate, $\Delta H_f(HCOO_{mon,ad}) = -(367 - 41\ \theta)$ kJ/mol, and bidentate formate, $\Delta H_f(HCOO_{bi,ad}) = -(410 - 74\ \theta)$ kJ/mol, where θ is the total number of HCOOH molecules adsorbed per Pt(111) surface atom. As discussed above, this reaction stoichiometry is best supported by spectroscopic data available in the literature.

We have also calculated these same enthalpies of formation assuming the formation of adsorbed water instead of the adsorbed water–hydroxyl complex, as given by

$$2HCOOH_g + O_{ad} \rightarrow 2HCOO_{ad} + H_2O_{ad} \quad (7)$$

The enthalpies of formation calculated with the stoichiometry from reaction 7 (red triangles in Figure 5) give enthalpies of formation that are more exothermic by ~5 kJ/mol, showing that the enthalpies of formate formation are quite insensitive to our proposal that the final structure of the H atom abstracted from the formic acid is as the water–OH complex instead of as simply adsorbed water. Nevertheless, we believe the literature is most consistent with the products represented by the upper curves (blue squares) in Figure 5.

We can use these enthalpies of formation determined here to predict the energetics of important elementary reactions such as the deprotonation of formic acid on clean Pt(111) to form adsorbed bidentate formate and a hydrogen adatom (H_{ad}), given by

$$HCOOH_{ad} \rightarrow HCOO_{bi,ad} + H_{ad} \quad (8)$$

By using the enthalpies of formation of bidentate formate at 0.375 ML (−382 kJ/mol), H_{ad} at zero coverage (−36 kJ/mol),[29] and formic acid gas (−379.2 kJ/mol) and the enthalpy of molecular adsorption of formic acid (−62.5 kJ/mol), the enthalpy of reaction 8 is found to be 24 kJ/mol *uphill* in energy (i.e., −382 + −36 − (−379.2 + −62.5) = 24 kJ/mol). However this reaction is *exothermic* by 4 kJ/mol using instead the enthalpy of formation of formate at the zero coverage limit. The shift from exothermic to endothermic occurs when the enthalpy of formation of formate is −406 kJ/mol at a coverage of 0.06 ML. Since monodentate formate is 30–40 kJ/mol less stable than bidentate formate (Figure 5), dehydrogenation of adsorbed formic acid to make monodentate formate plus H_{ad} is always endothermic, by ~40–50 kJ/mol depending on coverage.

The above enthalpies indicate that a much lower final coverage of formate can be expected on a clean Pt(111) surface than on a surface precovered with atomic oxygen. This is consistent with previous experiments that observed ~6–7 times lower coverages of adsorbed formate on the clean Pt(111) than on O-sat Pt(111).[16] These energetics show that the presence of a proton acceptor (e.g., O_{ad} or OH_{ad}) cause this deprotonation reaction to become a much more thermodynamically favorable process at low coverage and allow the deprotonation process to be remain exothermic at higher coverages.

As noted above, the lower initial total heat of adsorption at 190 K relative to the total heat at 150 K is due to the desorption of H_2O formed during reaction 6. As mentioned earlier, this difference, initially 15–20 kJ/mol at zero coverage, decreases with increasing formic acid coverage until 0.25 ML where the difference falls to zero. Above 0.25 ML, the heat of adsorption at 190 K falls sharply until the sticking probability reaches zero at ~0.31 ML. The decrease in the difference in the heats between the two temperatures coincides with a decrease in the intensity of the water desorption pulse seen in the mass spectrometer. This may indicate that adsorbed formate stabilizes the water hydroxyl complex, making decomposition of the complex slower at higher formate coverage. The sharp decrease in heat and lower saturation coverage at 190 K (0.31 ML) than at 150 K is likely due to competition between desorption and deprotonation of formic acid at 190 K. After one-quarter of surface sites are occupied, a formic acid molecule becomes increasingly more likely to desorb rather than deprotonate, consistent with the sticking data shown in Figure 1.

■ CONCLUSIONS

The enthalpies of formation of monodentate and bidentate formate on Pt(111) are −354 ± 5 and −384 ± 5 kJ/mol, respectively, at 3/8 ML coverage. The total formate–Pt(111) bond enthalpy in adsorbed monodentate formate is 224 ± 13 kJ/mol. The total bond enthalpy of bidentate formate to Pt(111) (two Pt–O bonds) is 254 ± 13 kJ/mol. The integral heat of adsorption of molecularly adsorbed formic acid on clean Pt(111) at 100 K is 62.5 kJ/mol at 0.25 ML. These enthalpies give the enthalpy of the reaction $HCOOH_{ad} \rightarrow HCOO_{bi,ad} + H_{ad}$ to be −4 kJ/mol at zero coverage and +24 kJ/mol at 0.375 ML. The first layer of molecularly adsorbed HCOOH saturates at a coverage of 0.5 ML at 100 K. Saturation coverages of

dx.doi.org/10.1021/ja412878u | J. Am. Chem. Soc. 2014, 136, 3964–3971

bidentate formate on O-sat Pt(111) at 150 and 190 K are 0.5 and 0.31 ML, respectively.

AUTHOR INFORMATION

Corresponding Author

campbell@chem.washington.edu

Notes

The authors declare no competing financial interest.

ACKNOWLEDGMENTS

The authors acknowledge support for this work by the National Science Foundation under CHE-1010287. We also wish to acknowledge John W. Heutink and Brian P. Holm at the Chemistry machine shop for their invaluable skill and expertise.

REFERENCES

(1) Grabow, L. C.; Gokhale, A. A.; Evans, S. T.; Dumesic, J. A.; Mavrikakis, M. *J. Phys. Chem. C* **2008**, *112*, 4608.
(2) Flaherty, D. W.; Yu, W.-Y.; Pozun, Z. D.; Henkelman, G.; Mullins, C. B. *J. Catal.* **2011**, *282*, 278.
(3) Sawada, T.; Liu, Z.; Takagi, N.; Watanabe, K.; Matsumoto, Y. *Chem. Phys. Lett.* **2004**, *392*, 334.
(4) Endo, M.; Matsumoto, T.; Kubota, J.; Domen, K.; Hirose, C. *Surf. Sci.* **1999**, *441*, L931.
(5) Endo, M.; Matsumoto, T.; Kubota, J.; Domen, K.; Hirose, C. *J. Phys. Chem. B* **2000**, *104*, 4916.
(6) Endo, M.; Matsumoto, T.; Kubota, J.; Domen, K.; Hirose, C. *J. Phys. Chem. B* **2001**, *105*, 1573.
(7) Miller, A. V.; Kaichev, V. V.; Prosvirin, I. P.; Bukhtiyarov, V. I. *J. Phys. Chem. C* **2013**, *117*, 8189.
(8) Barth, J. V.; Costantini, G.; Kern, K. *Nature* **2005**, *437*, 671.
(9) Sarikaya, M.; Tamerler, C.; Jen, A. K. Y.; Schulten, K.; Baneyx, F. *Nat. Mater.* **2003**, *2*, 577.
(10) Lynch, I.; Cedervall, T.; Lundqvist, M.; Cabaleiro-Lago, C.; Linse, S.; Dawson, K. A. *Adv. Colloid Interface Sci.* **2007**, *134*−*35*, 167.
(11) Kasemo, B. *Surf. Sci.* **2002**, *500*, 656.
(12) Grasemann, M.; Laurenczy, G. *Energy Environ. Sci.* **2012**, *5*, 8171.
(13) Cuesta, A.; Cabello, G.; Osawa, M.; Gutierrez, C. *ACS Catal.* **2012**, *2*, 728.
(14) Avery, N. R. *Appl. Surf. Sci.* **1983**, *14*, 149.
(15) Columbia, M. R.; Crabtree, A. M.; Thiel, P. A. *J. Electroanal. Chem.* **1993**, *351*, 207.
(16) Avery, N. R. *Appl. Surf. Sci.* **1982**, *11*−*2*, 774.
(17) Hodgson, A.; Haq, S. *Surf. Sci. Rep.* **2009**, *64*, 381.
(18) Lew, W.; Crowe, M. C.; Karp, E.; Lytken, O.; Farmer, J. A.; Arnadottir, L.; Schoenbaum, C.; Campbell, C. T. *J. Phys. Chem. C* **2011**, *115*, 11586.
(19) Borronibird, C. E.; King, D. A. *Rev. Sci. Instrum.* **1991**, *62*, 2177.
(20) Dixonwarren, S. J.; Kovar, M.; Wartnaby, C. E.; King, D. A. *Surf. Sci.* **1994**, *307*, 16.
(21) Stuckless, J. T.; Frei, N. A.; Campbell, C. T. *Rev. Sci. Instrum.* **1998**, *69*, 2427.
(22) Ajo, H. M.; Ihm, H.; Moilanen, D. E.; Campbell, C. T. *Rev. Sci. Instrum.* **2004**, *75*, 4471.
(23) Yeo, Y. Y.; Vattuone, L.; King, D. A. *J. Chem. Phys.* **1997**, *106*, 392.
(24) Fiorin, V.; Borthwick, D.; King, D. A. *Surf. Sci.* **2009**, *603*, 1360.
(25) Karp, E. M.; Silbaugh, T. L.; Crowe, M. C.; Campbell, C. T. *J. Am. Chem. Soc.* **2012**, *134*, 20388.
(26) Karp, E. M.; Silbaugh, T. L.; Campbell, C. T. *J. Phys. Chem. C* **2013**, *117*, 6325.
(27) Karp, E. M.; Silbaugh, T. L.; Campbell, C. T. *J. Am. Chem. Soc.* **2013**, *135*, 5208.
(28) Silbaugh, T. L.; Karp, E. M.; Campbell, C. T. *J. Catal.* **2013**, *308*, 114.
(29) Lew, W.; Lytken, O.; Farmer, J. A.; Crowe, M. C.; Campbell, C. T. *Rev. Sci. Instrum.* **2010**, *81*, 024102.
(30) Lytken, O.; Lew, W.; Harris, J. J. W.; Vestergaard, E. K.; Gottfried, J. M.; Campbell, C. T. *J. Am. Chem. Soc.* **2008**, *130*, 10247.
(31) Coolidge, A. S. *J. Am. Chem. Soc.* **1928**, *50*, 2166.
(32) Columbia, M. R.; Crabtree, A. M.; Thiel, P. A. *J. Am. Chem. Soc.* **1992**, *114*, 1231.
(33) Stuckless, J. T.; Frei, N. A.; Campbell, C. T. *Sens. Actuators, B* **2000**, *62*, 13.
(34) Lew, W.; Crowe, M. C.; Campbell, C. T.; Carrasco, J.; Michaelides, A. *J. Phys. Chem. C* **2011**, *115*, 23008.
(35) King, D. A.; Wells, M. G. *Surf. Sci.* **1972**, *29*, 454.
(36) Lew, W. D.; Crowe, M. C.; Karp, E.; Campbell, C. T. *J. Phys. Chem. C* **2011**, *115*, 9164.
(37) McCarty, J. G.; Madix, R. J. *Surf. Sci.* **1976**, *54*, 210.
(38) Campbell, C. T.; Sellers, J. R. V. *J. Am. Chem. Soc.* **2012**, *134*, 18109.
(39) Campbell, C. T.; Sellers, J. R. V. *Chem. Rev.* **2013**, *113*, 4106.
(40) Millikan, R. C.; Pitzer, K. S. *J. Chem. Phys.* **1957**, *27*, 1305.
(41) Ohtani, T.; Kubota, J.; Wada, A.; Kondo, J. N.; Domen, K.; Hirose, C. *Surf. Sci.* **1996**, *368*, 270.
(42) Chapman, D. *J. Am. Chem. Soc.* **1956**, 225.
(43) Stephenson, R. M.; Malanowski, S. *Handbook of the Thermodynamics of Organic Compounds*; Elsevier: New York, 1987.
(44) Sexton, B. A. *Surf. Sci.* **1981**, *102*, 271.
(45) Sexton, B. A.; Hughes, A. E.; Avery, N. R. *Surf. Sci.* **1985**, *155*, 366.
(46) Solymosi, F.; Kiss, J.; Kovacs, I. *Surf. Sci.* **1987**, *192*, 47.
(47) Barteau, M. A.; Bowker, M.; Madix, R. J. *Surf. Sci.* **1980**, *94*, 303.
(48) Lebedeva, N. D. *Russ. J. Phys. Chem.* **1964**, *38*, 1435.
(49) Karp, E. M.; Campbell, C. T.; Studt, F.; Abild-Pedersen, F.; Nerskov, J. K. *J. Phys. Chem. C* **2012**, *116*, 25772.
(50) Luo, Y.-R. *Comprehensive Handbook of Chemical Bond Energies*; CRC Press: Boca Raton, FL, 2007.